Wind tunnel wall corrections for unsteady flow applying steady wall adaptation and CFD-techniques

H. FÖRSCHING   (GÖTTINGEN)

WITH THE RECENT development of adaptive wind tunnel walls by which steady wall effects are eliminated or significantly reduced by actively controlling flow near the walls, new possibilities for correction of wind tunnel wall interference have also emerged for unsteady flow. In the present paper, prospects and concepts of experimental and analytical techniques for correction of unsteady wind tunnel wall effects, in the context of aerodynamic and aeroelastic wind tunnel investigation of oscillating lifting systems and bodies, are presented. First, some fundamental relations of motion-induced unsteady flow fields, basic to a physical understanding and analytical treatment of unsteady flow phenomena, are explained. Then the principal causes of unsteady wind tunnel interference are described and the practicability of adaptive wind tunnel walls to eliminate wall interference effects in aeroelastic wind tunnel model measurements is discussed. Finally prospective wind tunnel wall corrections for motion-induced unsteady flow, applying steady flow wall adaptation and advanced CFD-techniques, are outlined. Such a hybrid correction technique for 2D unsteady flow taking into account measured unsteady wind tunnel wall data from experiment to formulate precise tunnel wall boundary conditions is highlighted. Elaboration of such hybrid correction techniques is a challenging field of future aerodynamic research and would contribute substantially to a new generation of wind tunnel technology.

1. Introduction

WALL INTERFERENCE effects in aerodynamic wind tunnel investigations have been found to be a nuisance since the early days of such tests. Moreover, when flight speeds were beginning to approach transonic, and when it became necessary to perform wind tunnel tests at high subsonic and transonic Mach numbers, it was recognized that conventional solid wall wind tunnels became choked and that wall interference corrections based on linearized theory diverge as the test speed approaches Mach number one. An obvious solution was the contouring of the test section walls which led to early development of adaptive wall wind tunnels in the late 1930's. Another solution, that also goes back to the same time, was the development of test sections with ventilated (perforated or slotted) tunnel walls. The technical and operational simplicity of such ventilated wind tunnel test section walls soon led to the abandonment of the much more complicated adaptive approach. Hence, the ventilated wall concept then became the standard technique for high speed wind tunnel test sections, although some serious disadvantages had to be tolerated with this concept: the generation of aerodynamic noise and an increase in power by about 50% compared to a solid wall wind tunnel.

With the advent and the aid of high-speed computers new wind tunnel wall adaptation strategies became feasible to determine the exact, interference-free wall countour. Thus, since the early 1970's, a renewed interest in adaptive walls arose and great efforts have been made—and are still being made—to bring the computer-aided adaptive wind tunnel wall technology to practical maturity. At the present time many successful adaptive wall test sections are already operational for steady flow aerodynamic investigations.

With the recent development of such adaptive wall wind tunnel test sections, by which steady wall interference effects are eliminated or significantly reduced by actively control-

ling flow near the walls, new possibilities for correction of wind tunnel wall interference have also emerged for unsteady flow. However, in the case of unsteady flow, the wind tunnel wall interference problem is greatly complicated by additional parameters describing the typical time-dependent variation of the unsteady flow field. Moreover, other sources of interference, such as tunnel wall reflections in the form of acoustic waves and, as a consequence, wind tunnel resonance, may play an important role as well.

In the present paper, prospects and concepts of experimental and analytical techniques for the correction of unsteady wind tunnel wall effects, associated with aerodynamic and aeroelastic measurements of oscillating lifting systems and bodies, are presented. First, the basic concept of steady wind tunnel wall adaptation is briefly outlined and some fundamental relations of motion-induced unsteady flow fields, basic to a physical understanding and analytical treatment of unsteady flow phenomena, are explained. Then, the principal causes of unsteady wind tunnel interference are described and the practicability of adaptive wind tunnel walls to eliminate aerodynamic wall interference effects in unsteady aerodynamic and aeroelastic wind tunnel model measurements is discussed. Finally, prospective wind tunnel wall corrections for motion-induced unsteady flow, applying steady flow wall adaptation and advanced computational fluid dynamic (CFD) techniques, are outlined.

2. Basic concept behind wind tunnel wall adaptation

The basic concept behind wind tunnel wall adaptation is to match two independent flow-disturbance quantities measured at an interface (the tunnel wall) in the experiment to the same quantities computed from an interference-free flow outside the interface. If both quantities were to exhibit exactly the same value, then the contour of this interface would be equivalent to a streamline (or stream surface) in an unrestricted, interference-free flow field. This is shown schematically in Fig. 1, where the tunnel wall separates the inner, experimental flow region, II, from the outer computed flow region, I, which is actually just fictitious. For a real streamline the pressure on both sides of the interface must be the same: $p_I = p_{II}$. Hence, if the measured pressure p_{II} along the wall inside the tunnel coincides with the calculated pressure p_I for the fictitious flow over the known wall shape, $\varepsilon\eta(x,y)$, then the wall shape can be considered adapted. A principal feature of this adaptation concept is that there is no requirement for a theoretical representation of the flow about the test article.

Since any adjustment to the flow by means of wall control affects the entire flow field, both the inner, experimental flow and the outer, computational flow will change, i.e. adaptation becomes an iterative process.In the past years several such iterative adaptation strategies and relating streamlining algorithms have been elaborated, see Refs. [1–3] and have successfully been applied not only to actively controlled flexible wind tunnel walls but also to porous walls with variable suction, see Refs. [4, 5].

3. Basic physical relations of motion-induced unsteady flow fields

Before the applicability of adaptive walls in the case of unsteady flow is considered, some fundamental relations, basic to a physical understanding and computational treatment of unsteady flow phenomena, will first be explained in the following. In contrast to steady flow the differential equation that governs the inviscid compressible unsteady
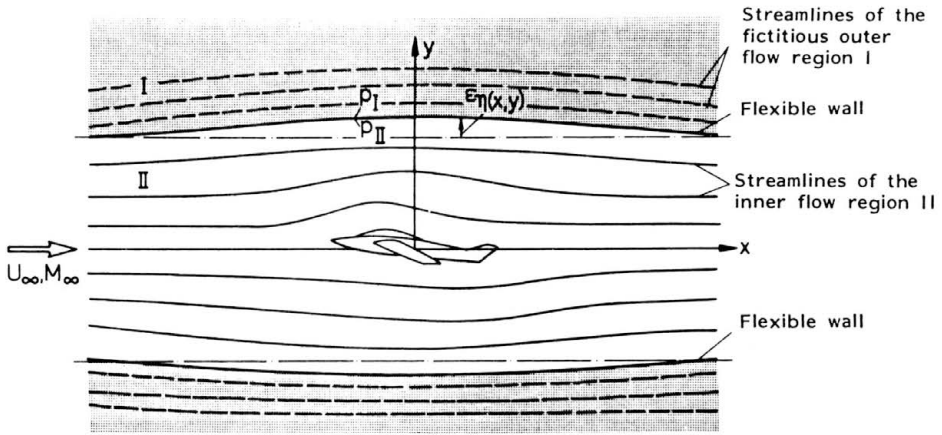
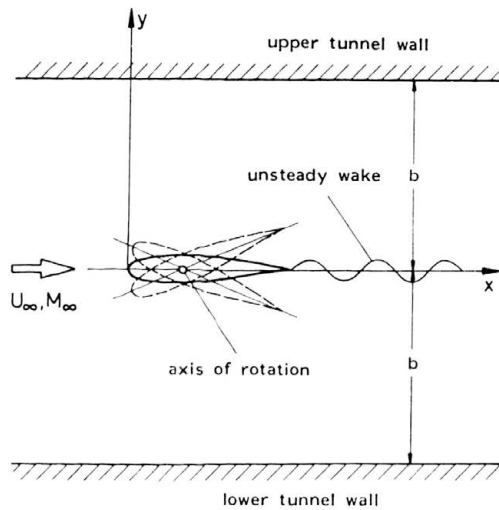FIG. 1. Principle of adaptive wind tunnel walls.

FIG. 2. Oscillating airfoil in a wind tunnel with coordinate system.

flow due to small oscillatory perturbations imposed on a steady, uniform flow field takes the form of a wave equation. In reference to rectangular coordinates, see Fig. 2, this equation in linearized form for two-dimensional unsteady compressible flow, generated by an oscillating airfoil, reads:

$$(3.1) \qquad (1 - M_\infty^2)\phi_{xx} + \phi_{yy} - 2\frac{M_\infty^2}{U_\infty}\phi_{xt} - \frac{1}{a_\infty^2}\phi_{tt} = 0.$$

Here, $\phi = \phi(x, y, t)$ is the time-dependent perturbation velocity potential, U_∞ the velocity of the undisturbed flow, M_∞ the corresponding Mach number and a_∞ the velocity of sound. When the steady free stream Mach number M_∞ is close to unity, the governing

equation for 2D transonic flow in its simplest form reads, see Ref. [6]:

$$(3.2) \qquad (1 - M_\infty^2)\phi_{xx} - (\gamma + 1)\frac{M_\infty^2}{U_\infty}\frac{\partial}{\partial x}(\phi_x^0\phi_x) + \phi_{yy} - 2\frac{M_\infty^2}{U_\infty}\phi_{xt} - \frac{1}{a_\infty^2}\phi_{tt} = 0,$$

where γ denotes the ratio of specific heats. Equation (3.2) is the time linearised transonic small perturbation (TSP) equation, where we recognize a nonlinear term associated with the steady flow potential ϕ^0 independent of time t.
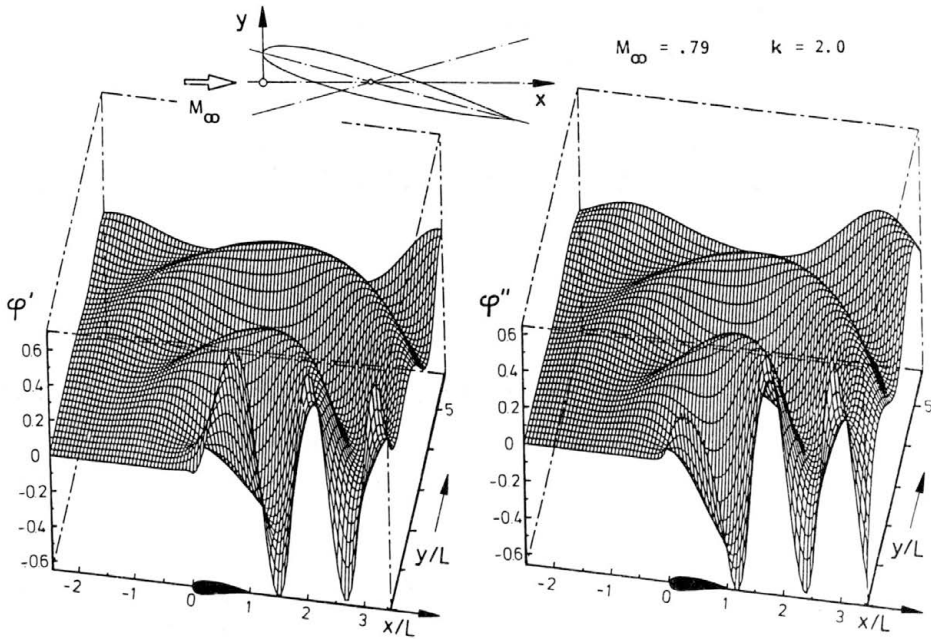

FIG. 3. Motion-induced unsteady flow field (complex unsteady potential function φ) of an airfoil performing harmonic pitching oscillations about the 0.425-chord axis (φ'—real part, φ''—imaginary part of φ).

In the case of harmonic motion of the airfoil,

$$(3.3) \qquad \phi(x, y, t) = \phi(x, y)e^{i\omega t},$$

with the coordinate transformations (L = reference length)

$$(3.4) \qquad \bar{x} = x/L, \quad \bar{y} = \beta y/L \quad \text{and} \quad T = \frac{tU_\infty}{L}, \quad \text{with} \quad \beta = \sqrt{1 - M_\infty^2},$$

and upon introduction of a reduced velocity potential φ,

$$(3.5) \qquad \phi = \varphi e^{i\varepsilon\bar{x}},$$

Eq. (3.1) can be transformed into the well-known Helmholtz wave equation:

$$(3.6) \qquad \varphi_{\bar{x}\bar{x}} + \varphi_{\bar{y}\bar{y}} + \lambda^2\varphi = 0.$$

A fundamental solution of Eq. (3.6) is

$$(3.7) \qquad \varphi \sim H_0^{(2)}(\lambda r),$$

where

$H_0^{(2)}$ Hankel function of second kind and order zero, satisfying the Sommerfeld radiation condition,

k $\dfrac{\omega L}{U_\infty}$ — reduced frequency (ω — circular frequency),

λ $\dfrac{k M_\infty}{\beta^2}$ — reduced wave number,

ε λM_∞, and

r $\sqrt{(\overline{x} - \overline{\xi})^2 + (\overline{y} - \overline{\eta})^2}$ — distance between transmitting $(\overline{\xi}, \overline{\eta})$ and receiving field point.

Hence, the unsteady part of the flow field of a harmonically oscillating airfoil may be represented by a superposition of perturbation sources which move with the base flow velocity U_∞ and propagate in the form of waves with the velocity of sound a_∞, thus exhibiting a waviness of the flow field dependent on the parameters λ and/or ε and on the mode of oscillation as well. As a typical example, Fig. 3 illustrates the motion-induced unsteady flow field of an oscillating airfoil in 2D compressible flow, where φ' denotes the real part (in phase with the oscillating airfoil) and φ'' the imaginary part (90 degrees out of phase) of the unsteady velocity potential φ. It can be seen in Fig. 3 that this unsteady flow field is by far more complicated than the steady flow field of an airfoil at rest.

4. Wind tunnel interferences in unsteady flow

From the practical point of view, the most important types of motion-induced unsteady flow fields in a wind tunnel arise from forced or self-excited (flutter) oscillations of the (elastic) model. In such wind tunnel investigations the unsteady aerodynamic data of main interest are the magnitude and phase of the motion-induced unsteady aerodynamic pressures. For instance, for an airfoil performing a pitching oscillation of amplitude Θ about a mean incidence α_0, the wall interference effects on magnitude and phase of the unsteady pressures can be considered under the following headings:

1) *steady* effects on the flow for the mean incidence α_0,

2) *quasi-steady* effects in context with the time-dependent kinematic flow conditions for all changes of incidence within the range $(\alpha_0 - \Theta) < \alpha < (\alpha_0 + \Theta)$,

3) *unsteady* effects on the manner in which the magnitude and phase of the motion-induced unsteady pressure vary with frequency in context with the unsteady wake.

Hence, the requirements for avoidance of wind tunnel wall interference effects on unsteady measurements are:

1) correct (undisturbed) base flow and correct steady perturbations,

2) absence of any additional unsteady effects,

i.e. an unsteady process may be directly affected by steady flow wall interference as well as by the purely unsteady sources of interference.

The principal causes of unsteady tunnel interference—in addition to the well-known steady interference effects, such as wall constraint, shock wave reflection in transonic flow and wall boundary layers—are, see Fig. 4:

1) unsteady effects of wall constraint,

2) reflection by the walls of model-generated acoustic disturbances, and—as a consequence—acoustic wind tunnel resonance,

3) distortion of the oscillatory wake of the model by other tunnel deficiencies,
4) inherent tunnel flow fluctuations.

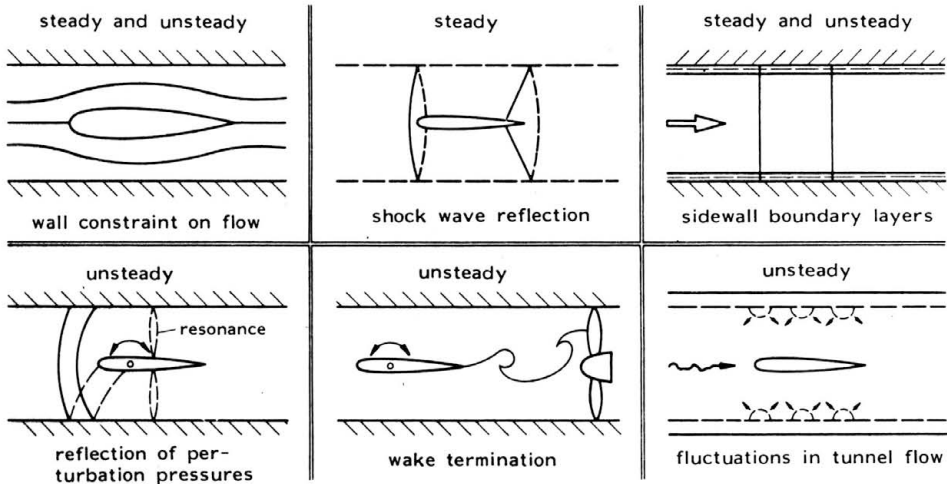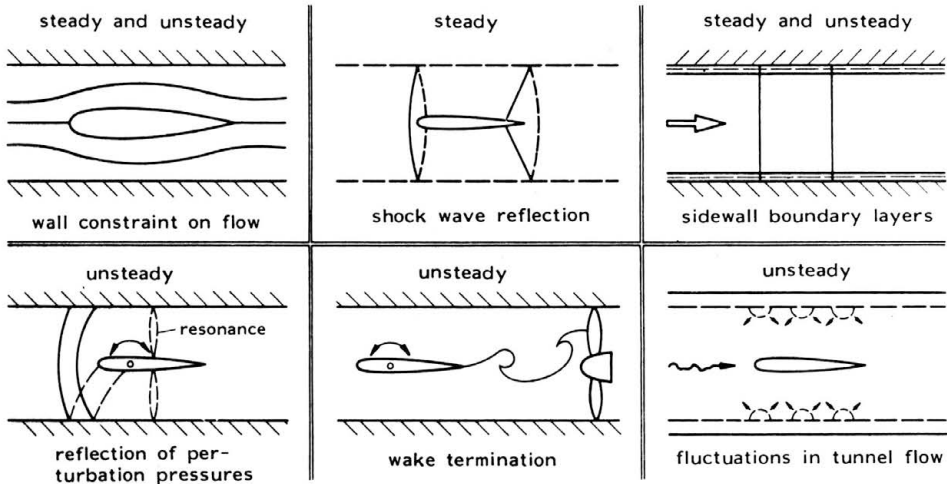| steady and unsteady	steady	steady and unsteady
wall constraint on flow	shock wave reflection	sidewall boundary layers
unsteady	unsteady	unsteady
reflection of per-turbation pressures	wake termination	fluctuations in tunnel flow

FIG. 4. Principal causes of wind tunnel interference.

Since a clear understanding of these unsteady wind tunnel interference effects is of basic concern for the application of adaptive wall concepts, they will be discussed in more detail in the following.

Corrections for unsteady effects of wall constraint—excluding transonic flow—in tunnels having well-defined wall boundary conditions can readily be obtained from theoretical investigations. The corresponding boundary conditions for open and closed (solid) wind tunnel walls can easily be established, but it is difficult to obtain quantitative estimates for ventilated wind tunnel walls because of mathematical uncertainties about the boundaries. For two-dimensional airfoils oscillating in sub- and supersonic flow several such analytical unsteady wall correction techniques have already been elaborated, see Refs. [7–12].

Reflection of acoustic disturbances from wind tunnel walls and their return to the model is a crucial unsteady interference problem. As shown in the previous section, an oscillating model generates unsteady pressure disturbances in the form of travelling acoustic waves which propagate outwards in the tunnel. After being reflected from the walls, these disturbances return to the model causing additional pressure changes there. This is in contrast to the Sommerfeld far-field radiation condition which requires a reflection-free propagation of the disturbances to infinity in free atmosphere. Figure 5 shows an airfoil in 2D subsonic flow and the wave fronts from an acoustic disturbance in a uniform flow. It is seen that the velocity of propagation of the pressure disturbance from a point P_0 in the direction normal to the wall is $\sqrt{a_\infty^2 - U_\infty^2}$, and the time needed for the disturbance to be reflected by the wall and return to P_0 is

$$(4.1) \qquad \Delta t = 2b/\sqrt{a_\infty^2 - U_\infty^2} = 2b/\beta a_\infty,$$

where b is the distance to the wall. The attenuation of the disturbance by the time it returns to the source will depend on the distance travelled in the moving air which is

$$(4.2) \qquad a_\infty \Delta t = 2b/\beta.$$

3) distortion of the oscillatory wake of the model by other tunnel deficiencies,
4) inherent tunnel flow fluctuations.

steady and unsteady	steady	steady and unsteady
wall constraint on flow	shock wave reflection	sidewall boundary layers
unsteady	unsteady	unsteady
reflection of per-turbation pressures	wake termination	fluctuations in tunnel flow

FIG. 4. Principal causes of wind tunnel interference.

Since a clear understanding of these unsteady wind tunnel interference effects is of basic concern for the application of adaptive wall concepts, they will be discussed in more detail in the following.

Corrections for unsteady effects of wall constraint—excluding transonic flow—in tunnels having well-defined wall boundary conditions can readily be obtained from theoretical investigations. The corresponding boundary conditions for open and closed (solid) wind tunnel walls can easily be established, but it is difficult to obtain quantitative estimates for ventilated wind tunnel walls because of mathematical uncertainties about the boundaries. For two-dimensional airfoils oscillating in sub- and supersonic flow several such analytical unsteady wall correction techniques have already been elaborated, see Refs. [7–12].

Reflection of acoustic disturbances from wind tunnel walls and their return to the model is a crucial unsteady interference problem. As shown in the previous section, an oscillating model generates unsteady pressure disturbances in the form of travelling acoustic waves which propagate outwards in the tunnel. After being reflected from the walls, these disturbances return to the model causing additional pressure changes there. This is in contrast to the Sommerfeld far-field radiation condition which requires a reflection-free propagation of the disturbances to infinity in free atmosphere. Figure 5 shows an airfoil in 2D subsonic flow and the wave fronts from an acoustic disturbance in a uniform flow. It is seen that the velocity of propagation of the pressure disturbance from a point P_0 in the direction normal to the wall is $\sqrt{a_\infty^2 - U_\infty^2}$, and the time needed for the disturbance to be reflected by the wall and return to P_0 is

$$(4.1) \qquad \Delta t = 2b/\sqrt{a_\infty^2 - U_\infty^2} = 2b/\beta a_\infty,$$

where b is the distance to the wall. The attenuation of the disturbance by the time it returns to the source will depend on the distance travelled in the moving air which is

$$(4.2) \qquad a_\infty \Delta t = 2b/\beta.$$

Thus the reflected wave when it returns will be weaker (by natural damping), the higher the Mach number. When a disturbance from the oscillating airfoil is reflected from the tunnel wall back to the wing with such a phase relationship that it reinforces, or cancels out, a succeeding disturbance and hence the pressure changes currently occurring on the model, then we have the case of acoustic resonance. This certainly is the most severe unsteady wall interference problem, first described in Ref. [13] and experimentally verified in Ref. [14]. For solid walls, that do not change the phase of the wave on reflection, the resonance circular frequency is

(4.3) $$\omega_n = (2n - 1)\pi U_\infty \frac{\beta}{M_\infty} \frac{1}{2b}, \quad n = 1, 2, \dots .$$

For open jet boundaries the phase change on reflection is π, so that

(4.4) $$\omega_n = 2n\pi U_\infty \frac{\beta}{M_\infty} \frac{1}{2b}, \quad n = 1, 2, \dots .$$

For a tunnel with ventilated walls, theoretical expressions for the resonance frequencies depending on wall porosity, depth of plenum chamber and Mach number are given in Ref. [15]. In the case of resonance, where the disturbances form a standing wave pattern, the normal velocity has a maximum amplitude and the pressure has a node, i.e. is of zero amplitude at the position of the oscillating airfoil. Accordingly, the unsteady airloads on the oscillating airfoil will vanish at resonance. A typical example is shown in Fig. 6. Whereas for incompressible flow ($M_\infty \to 0$) there is no tunnel resonance—the resonance frequency decreases with increasing Mach number—and since it tends to zero as $M_\infty \to 1$, the predicated resonance frequency must coincide with a test frequency for some intermediate Mach number causing dramatic changes in the magnitude and phase of the unsteady lift on the oscillating model. Fortunately at the higher Mach numbers there are influences to reduce these effects. Even for strong reflections from solid walls, the effective air distance travelled increases with Mach number and the reflections thus become more attenuated. Also, the reflected disturbances travel more with the flow than across it, see Fig. 5. Furthermore, for transonic conditions, when the resonance frequencies are low enough, the (adapted) walls in typical transonic wind tunnels will be perforated or slotted and the reflections thus more diffuse and attenuated.

In a free atmosphere an oscillating model would leave behind an oscillating wake the vorticity distribution of which is consistent with the unsteady flow at the model. If in a tunnel this wake is affected by a tunnel shock wave, the driving fan or a near tunnel corner, the unsteady aerodynamic loading at the model may be notably influenced. There are reasons to suggest that this source of unsteady interference is of considerable importance in certain special cases of low flow speed and less important in transonic flow.

Finally, various types of flow fluctuations, often described collectively as *tunnel noise*, can have several unwanted effects, particularly in aeroelastic model investigations. One of the principal sources of noise in transonic tunnels is the flow over ventilated walls. It is possible to reduce the noise from this source by covering the perforations with gauze cloth and to apply sound-absorbing material to the tunnel walls, as shown in Ref. [16].

5. Application of adaptive wind tunnel walls in unsteady flow

From the preceding explanations we have seen that the following wind tunnel interference effects, due to an unsatisfactory test environment, are of main concern in unsteady

aerodynamic and aeroelastic experiments with oscillating models:

1) interference of the steady base flow field by steady wall constraints, including shock wave reflections in transonic flow,

2) interference of the (superimposed) motion-induced unsteady flow field by wall constraints,

3) reflection of the model-generated acoustic disturbances by the walls,

4) acoustic tunnel resonance in the test section.

With regard to the application of adaptive wind tunnel wall concepts to eliminate or significantly reduce these wall interference effects in unsteady flow measurements, the following statements can be made.

Ad 1.

Practicability and feasibility of wall adaptation for steady flow have already successfully been demonstrated in many wind tunnels. At least for free stream subsonic flow, in which locally supersonic regions may occur near the model, wall adaptation can be incorporated with confidence in the design and construction of future wind tunnels.

Ad 2.

Unsteady wall adaptation can be realized, at least theoretically, in the same way as for steady flow conditions. However, enormous technical effort is mandatory even for 2D-measurements. Unsteady wall adaptation would require oscillatory moving flexible walls, where the motion of the walls and the wall contours would depend on the frequency and vibration mode of the model, on the model amplitude of oscillation and on certain phase relationships with respect to the motion of the model. Streamlining algorithms for such a nonstationary wall adaptation, even for the simplest case of non-flexible (rigid body) oscillations of the model, would be very difficult to establish. 3D adaptive walls lie beyond the realm of practicability.

Ad 3.

Elimination would demand basically the same techniques and requirements as for nonadaptive walls, i. e. ventilated walls to diminish the reflections and a model-to-tunnel size-ratio as small as possible.

Ad 4.

Remains essentially unaffected by adaptive walls and cannot completely be eliminated by any type of tunnel wall.

Summarizing it can be stated that the elimination or at least reduction of unsteady wind tunnel wall interference by means of adaptive walls is extremely difficult to realize, if not even impossible. Unsteady wall adaptation, therefore, cannot be considered to be a reasonable means to overcome this problem. However, since unsteady aerodynamic processes may also strongly be affected by steady flow wall interferences, particularly in the transonic flow regime, avoidance of steady flow wall effects by application of steady flow wall adaptation could also significantly improve the results of unsteady wind tunnel measurements, as demonstrated in Ref. [17] and shown in Fig. 7. Indeed, the application of adaptive walls to minimize interference from steady flow wall constraints, together with the application of advanced CFD-techniques which take into account unsteady wall pressure data from experiments to describe precise wall boundary conditions, is most promising in deriving corrections for wind tunnel wall interferences in unsteady flow. Prospects and concepts for such hybrid wind tunnel wall correction techniques are outlined in the following.
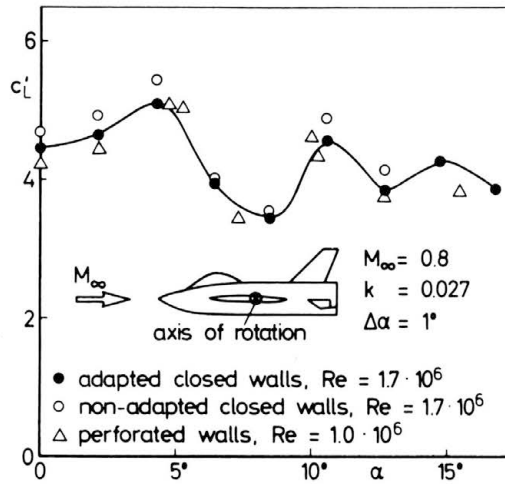
FIG. 7. In-phase-component c'_L of unsteady lift coefficient of a harmonically oscillating model with and without steady closed tunnel wall adaptation and with perforated walls (adapted from Ref. [17]).

6. Wind tunnel wall corrections for unsteady flow applying steady wall adaptation and CFD-techniques

6.1. Prediction methods for 2D unsteady wall interference

Analytical predictions of wall effects on unsteady pressures and airloads require exact knowledge of the wall boundary conditions. Only three types of boundary conditions are well-defined, namely those of solid (closed) walls, free jet and of prescribed unsteady wall pressure distributions (known from experiment). Porous or slotted walls can be simulated only approximately by mixed boundary conditions including free parameters. Until now systematic theoretical studies of unsteady wall effects have only been carried out for 2D airfoils oscillating in subsonic and supersonic flow. As wind tunnel test s with oscillating models are performed primarily for aeroelastic purposes, wind tunnel interference effects have to be studied within a wide range of Mach numbers, oscillation modes and reduced frequencies.

For 2D subsonic flow in one of the first systematic analytical investigations on wind tunnel wall effects, based on Eq. (3.1) BLAND [7] derived an integral equation relating the downwash w (prescribed by the harmonic motion of the airfoil) to the induced unsteady pressure jump δp at the airfoil:

$$(6.1) \qquad w(\overline{x}) = \int_0^1 K(\overline{x} - \overline{\xi}, M_\infty, k)\delta p(\overline{\xi})d\overline{\xi}.$$

This is an extension of Possio's integral equation [18], which is valid for free stream conditions. Bland derived the rather complicated kernel K by Fourier transformation, including tunnel wall boundary conditions to be automatically fulfilled on infinitely extended walls

in the general form:

$$(6.2) \qquad p \pm c_w \frac{\partial p}{\partial y} = 0, \quad \text{at} \quad y = \pm b \binom{\text{upper}}{\text{lower}} \text{walls},$$

where c_w denotes a specific wall parameter. The limiting cases of solid walls and free jet are included in Eq. (6.2), when

$$(6.3) \qquad \begin{array}{ccccccc} c_w = 0 & \rightarrow & p = 0 & \rightarrow & \varphi = 0 & \text{(free jet)}, \\ c_w = \infty & \rightarrow & \partial p / \partial \overline{y} = 0 & \rightarrow & \partial \varphi / \partial \overline{y} = 0 & \text{(closed wall)}. \end{array}$$

Thus, the effects of ventilated walls are described by certain values of c_w, but the dependence of c_w upon the kind of walls, their opening ratio and perhaps Mach number and reduced frequency is unclear and would have to be studied systematically by comparison with experiments.

Bland's method was completed by FROMME and GOLBERG [8, 9], who improved the numerical performance of the solution method and extended it to general oscillation modes, including flap motions. They obtained results showing clearly the unsteady wall effects, especially the sharp drops in magnitude of the loads and their phase jumps in the case of acoustic resonance, see Fig. 8. Wall effects are significant in the whole frequency regime and wall-influenced loads are bigger/smaller than the corresponding free stream values for closed/open walls, which is well-known for steady or quasi-steady flow. In particular, the strong changes in phase deserve special attention.
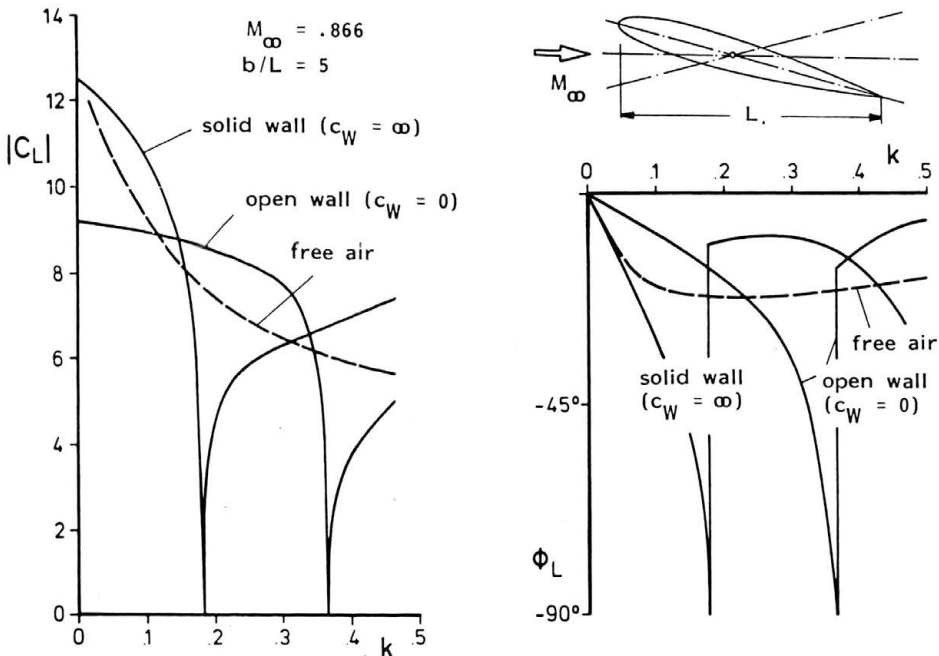

FIG. 8. Lift coefficient $|c_L|$ and phase angle ϕ_L of an airfoil performing harmonic pitching oscillations about the 0.5-chord axis in the case of acoustic resonance (adapted from ref. [8]).

This numerical method provides exact reference results, but it is restricted to 2D flows and to the regime of linear compressibility, i.e. constant Mach number in the whole flow field. It hardly appears possible to extend this method to 3D or transonic flow.
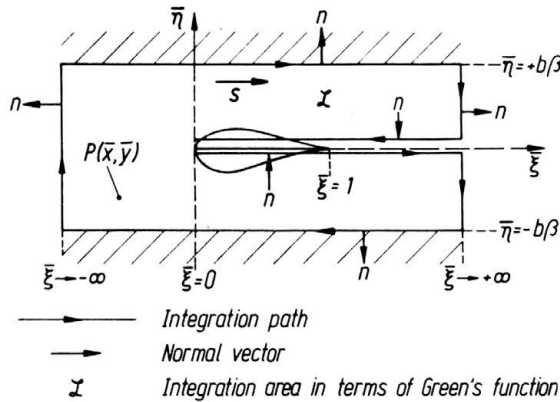
FIG. 9. Integration path and integration area applying Green's theorem
for the solution of Eq. (3.1).

The following numerical approach, elaborated recently at DLR/Göttingen and pub-
lished in Ref. [19], is more flexible. It is also based on the 2D linear Eq. (3.1), but
can be extended to 3D and even transonic flow as shown later. Within the framework
of linearised unsteady theory (small amplitudes of oscillation) the position of the airfoil,
its wake and the walls may be assumed to be approximately parallel to the x-axis, see
Fig. 2. The airfoil is located midway between the tunnel walls, a distance b away from
them. Then, as fully described in Ref. [19], this 2D boundary problem can be solved by
application of Green's theorem:

$$(6.4) \qquad \varphi(\overline{x}, \overline{y}) = \oint_C (\psi \frac{\partial \varphi}{\partial n} - \varphi \frac{\partial \psi}{\partial n}) ds = 0.$$

Here,

$$(6.5) \qquad \psi = \frac{1}{4i} H_0^{(2)}(\lambda r), \qquad r = \sqrt{(\overline{\xi} - \overline{x})^2 + (\overline{\eta} - \overline{y})^2},$$

is Green's function which satisfies Eq. (3.6) and Sommerfeld's far-field radiation condition
according to Eq. (3.7). The integration contour C and the integration path s run along the
boundaries of the control volume and along those boundaries where φ is discontinuous,
see Fig. 9. For free flight conditions, infinite boundaries have no effect. Thus, only the
profile contour and the wake line have to be taken into account. For flows in a wind tunnel
the integration path also has to run along the tunnel walls. As a final result one obtains an
analytical relationship between the downwash w at the airfoil, which is prescribed by the
airfoil's oscillatory motion, and the unsteady potential value f and the normal unsteady
velocity component g at the walls,

$$(6.6) \qquad \begin{cases} w = \partial \varphi / \partial \overline{y} & \text{at the profile,} \\ f = \varphi & \text{on the walls,} \\ g = \partial \varphi / \partial \overline{y} & \text{on the walls,} \end{cases}$$

in terms of the following set of integral equations:

(6.7)
$$\begin{cases} w = A\delta\varphi + A_1 f + A_2 g, \\ f = B_0^{-1}(B\delta\varphi + B_1 g), \\ g = C_0^{-1}(c\delta\varphi + C_1 f). \end{cases}$$

These equations relate the downwash distribution w to an unknown dipole distribution $\delta\varphi$, which provides the unsteady pressure jump at the airfoil by taking the unsteady flow values f and g at the windtunnel walls into account. A, A_1, A_2, B_0, B, B_1 and C_0, C, C_1 are known integral operators (kernel functions).

For the numerical solution of Eq. (6.7) the wing profile and the walls are divided into line elements (panels) on which w, $\delta\varphi$, f, g are approximately constant for each discrete step. The dipole strength in the wake in subsonic flow is approximated by the values near the trailing edge and by use of the Kutta condition. Since the unsteady potential function, especially downstream of the airfoil, decreases only slowly, see Fig. 3, the control area of the integral equation should be extended over several chords (at least 10 upstream and 10 downstream, as numerical test have shown). Applying this panel technique, or any other straight-forward CFD-technique for the numerical solution of Eqs. (6.7), the latter will be transferred to a corresponding system of linear algebraic equations, where A, A_1, A_2, B_0, B, B_1, C_0, C, C_1 are now the known aerodynamic influence coefficient matrices replacing the integral operators, and where w, $\delta\varphi$, f, g are now column vectors of the corresponding values at the airfoil and at the wall control points. For the cases of solid and open walls, Eqs. (6.7) simplify to the closed forms,

(6.8)
$$\text{solid walls}: \quad g = 0 \rightarrow w = (A + A_1 B_0^{-1} B)\delta\varphi,$$
$$\text{open walls}: \quad f = 0 \rightarrow w = (A + A_2 C_0^{-1} C)\delta\varphi,$$

from which the (wall-affected) potential jumps $\delta\varphi$, and hence the related unsteady pressures, can be calculated for a prescribed downwash w, i.e. oscillatory motion of the airfoil.

In Figs. 10–11 some typical results obtained from this numerical method are illustrated. Figs. 10 and 11 show the wall-influenced and free stream pressure jumps in terms of the complex unsteady pressure coefficient $\Delta c_p = (p_{\text{upper}} - p_{\text{lower}})/(q_\infty \cdot \Delta\alpha)$ (with q_∞ = free stream dynamic pressure and $\Delta\alpha$ = pitching amplitude) on a 2D plate, performing harmonic pitching oscillations about the 0.425-chord axis, and on an oscillating flap for the same Mach number M_∞, reduced frequency k and wall distance b/L. Again it can be seen that solid walls increase the loads while open walls produce the opposite effect. Figure 12 shows the pressure jump Δc_p for the same conditions as in Fig. 10, except that the reduced frequency has been changed so that it is close to the first solid wall resonance frequency. It can be seen that both the real part $\Delta c_p'$ and the imaginary part $\Delta c_p''$ are nearly zero in the case of the solid wall.

6.2. Application of numerical methods for correction of 2D experimental results

If it is possible to measure the unsteady wall pressure distributions during the test, they can be used to correct the wall-influenced unsteady pressure data at the model to corresponding freestream values. Such wall pressure measurements are a basic requisite in all steady flow adaptive wall concepts. In this case unsteady wall pressure data (in amplitude and phase) can also readily be measured. Then the afore-mentioned numerical correction technique can be applied in the way described in Ref. [19] as follows.
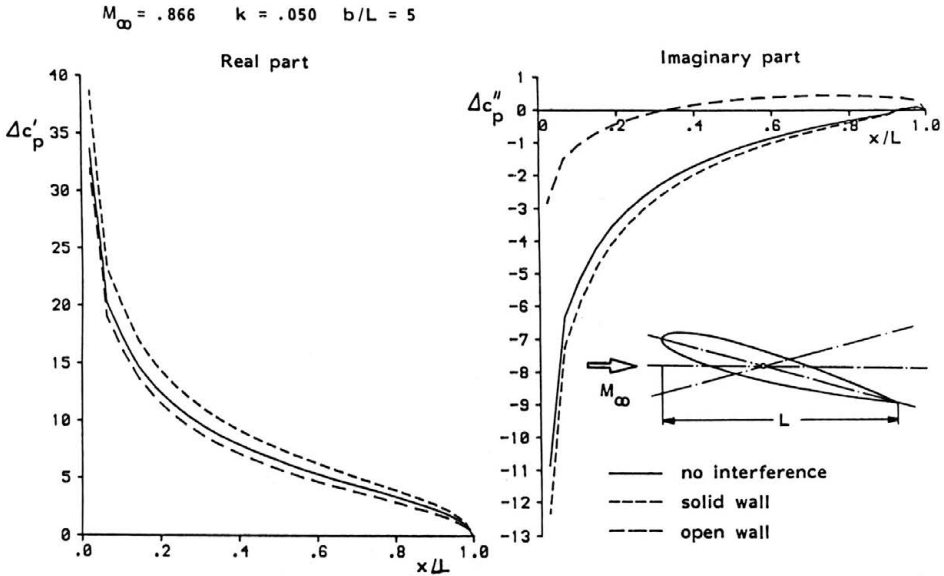
$M_\infty = .866$ $k = .050$ $b/L = 5$

FIG. 10. Complex unsteady pressure coefficient Δc_p of an airfoil performing harmonic pitching oscillations about the 0.425-chord axis at different wall conditions.

From the experimental unsteady (harmonic) wall pressure distributions c_P^W the corresponding potentials φ^W at the walls can be obtained from

$$(6.9) \qquad c_P^W = -2\left(\varphi_{\overline{x}}^W + i\frac{k}{\beta^2}\varphi^W\right)e^{i\varepsilon\overline{x}}$$

and hence

$$(6.10) \qquad \varphi^W = -\frac{1}{2}\int_{-\infty}^{\overline{x}} c_P^W(\overline{\xi})\exp\left[i\left(k\overline{\xi} - \frac{k}{\beta^2}\overline{x}\right)\right]d\overline{\xi}.$$

The wall pressures have to be measured at enough points upstream and downstream of the model within the area of integration. Then from Eqs. (6.7), one obtains an integral equation for the wall-affected dipole distribution $\delta\varphi^*$ on the model:

$$(6.11) \qquad (A + A_2 C_0^{-1} C)\delta\varphi^* = w - (A_1 + A_2 C_0^{-1} C_1)\varphi^W,$$

or

$$(6.12) \qquad A_1^* \delta\varphi^* = w - A_2^* \varphi^W = w - w^W.$$

It can be seen that the wall effects change the downwash and the kernel of the integral equation, compared to the corresponding free stream equation

$$(6.13) \qquad A\delta\varphi = w.$$

Substitution of Eq. (6.13) in (6.12), finally, yields the following integral equation:

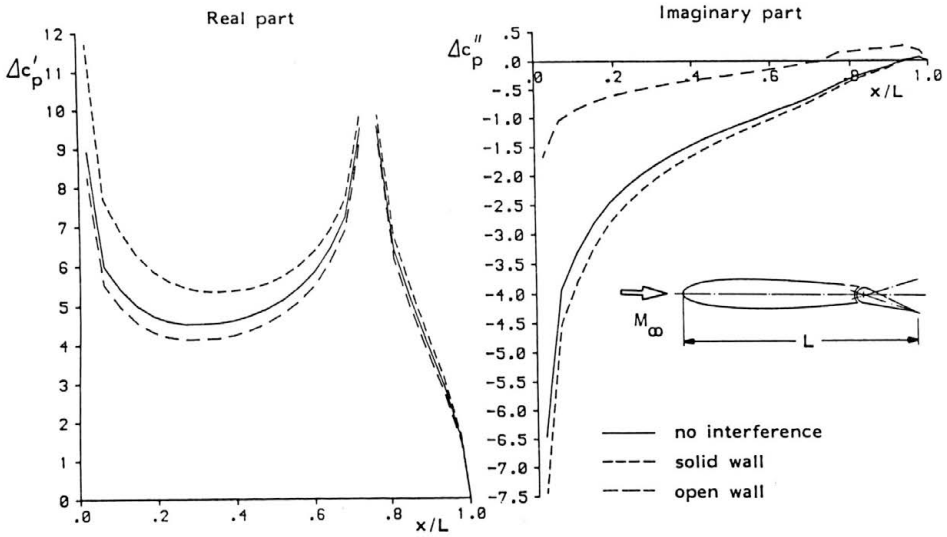$$(6.14) \qquad A_1^* \delta\varphi^* = A\delta\varphi - A_2^* \varphi^W,$$

FIG. 11. Complex unsteady pressure coefficient Δc_p of an airfoil
with harmonically oscillating flap at different wall conditions.
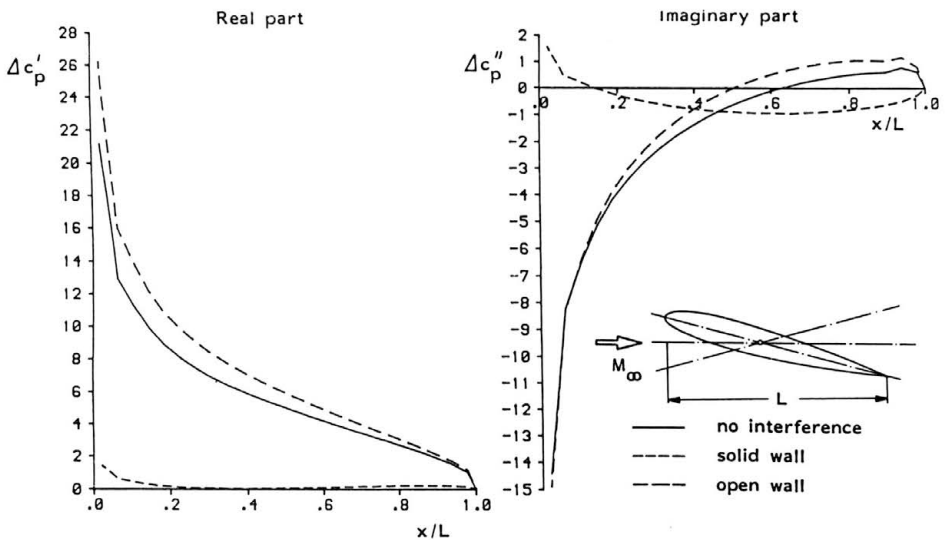

FIG. 12. Complex unsteady pressure coefficient Δc_p of an airfoil performing harmonic pitching oscillations
about the 0.425-chord axis at a reduced frequency k close to the first solid wall resonance condition.

in which the kernel functions (influence coefficient matrices) A, A_1^* and A_2^* are known from theory; $\delta\varphi^*$ (and hence Δc_P^*) on the model and φ^W at the wind tunnel walls (see Eq. (6.10)) are known from experiment. Thus, Eq. (6.14) can be used for correction of the measured wall-influenced Δc_P^*-distributions on the model in order to obtain the corresponding free stream values $\delta\varphi$ or Δc_P, respectively. Numerical solution of Eq. (6.14) can again be performed by means of advanced CFD-techniques.

It should be mentioned that SAWADA [12] arrived in his correction technique, where he also applied Green's theorem, at a formulation similar to Eq. (6.14). The advantage of his approach is, that the pressure distributions at the walls and at the model appear directly in his integral equations. But the kernels of these equations are rather complicated functions. The results he obtained are encouraging for low frequencies but are not as good in the vicinity of the resonance frequencies. Nevertheless, for 2D subsonic flow, this could be a promising unsteady wall correction procedure, but an extension to 3D and transonic flow and to more complicated (elastic) mode shapes of the oscillating model appears to be extremely difficult. Finally, for the sake of completeness, it should be mentioned that Jones in his 2D correction technique, see Ref. [20], took the walls into account by an infinite series of image singularity distributions by which he derived a correction technique for wall interference in subsonic flow.

6.3. Extension to 2D transonic flow

An extension of the correction method described in Ref. [19] to 2D transonic flow is possible, if

a) the unsteady flow field may still be treated as a small harmonic disturbance of the steady transonic flow field (i.e. small amplitude of harmonic oscillations),

b) the steady transonic flow field is well adapted (no steady wall interference) and known the extension of supersonic regions in the wind tunnel test section is significantly smaller than the wall distance from the model.
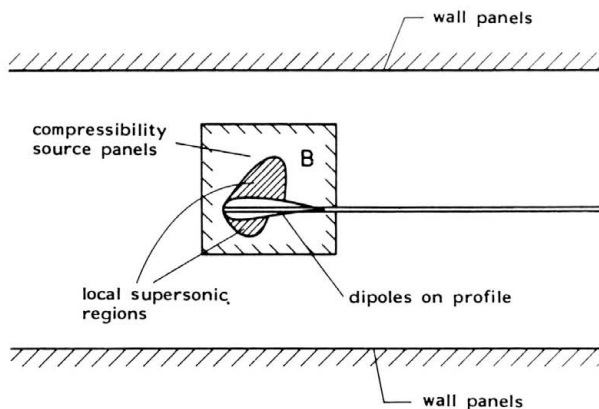

FIG. 13. Region of integration for the solution of the transonic 2D boundary value problem including the additional near-field control area B.

From a) it follows, that the unsteady flow may be described by a complex velocity

potential amplitude function ϕ which is governed by the time linearised TSP-equation (3.2). Then, for harmonic oscillations according to Eq. (3.3) and applying the transformations expressed by Eqs. (3.4) and (3.5), the TSP-equation (3.2) takes the form of an inhomogeneous Helmholtz equation:

$$(6.15) \qquad \varphi_{\bar{x}\,\bar{x}} + \varphi_{\bar{y}\,\bar{y}} + \lambda^2 \varphi = \left(\frac{\partial}{\partial \bar{x}} + i\varepsilon \right) \left((\gamma + 1) \frac{M_\infty^2}{\beta^2} \phi_{\bar{x}}^0 (\varphi_{\bar{x}} + i\varepsilon\varphi) \right) = S(\varphi).$$

A direct integral equation method for the solution of this equation under free stream conditions is described in Ref. [21]. This numerical computation technique can equally be applied to provide corrections for 2D unsteady transonic wall effects, where a wall-interference-free steady transonic flow (by application of adaptive walls) would be a prerequisite. Figure 13 shows the region of integration for this transonic boundary value problem. The additional near-field control area B comprises the local supersonic regions and can be represented by a rather limited number of additional unknowns. Then, an integral equation problem can be formulated for closed walls as well as for the free stream condition, and hence for their difference, which is the potential of the desired correction:

$$(6.16) \qquad \int_0^\infty \delta(\varphi - \varphi^f)\psi_{\bar{\eta}\,\bar{\eta}}d\bar{\xi} - \iint_B S(\varphi - \varphi^f)\psi_{\bar{\eta}}df = - \int_{-\infty}^\infty \varphi^w \psi_{\bar{\eta}\,\bar{\eta}}d\bar{\xi}$$

on the profile and

$$(6.17) \qquad \int_0^\infty \delta(\varphi - \varphi^f)\psi_{\bar{\eta}}d\bar{\xi} + (\varphi - \varphi^f) - \iint_B S(\varphi - \varphi^f)\psi df = - \int_{-\infty}^\infty \varphi^w \psi_{\bar{\eta}}d\bar{\xi}$$

in field control points of B, where φ^f denotes the free stream disturbance potential. Eqs. (6.16) and (6.17) can be solved by the numerical method described in Ref. [21]. For ventilated walls the integral equation would also contain normal velocity terms at the walls. These terms would have to be eliminated by mixed boundary conditions as formulated in Eq. (6.2) by introducing the unknown wall parameter c_w.

6. 4. Extension to 3D problems and application of finite difference methods

In Ref. [22] GARNER *et al.* developed a 3D correction method for ventilated tunnel walls by describing the wall influences through an infinite series of images of the vortex distributions representing the model. This method has been modified in Ref. [17] by using experimental unsteady pressures at closed tunnel walls which have been adapted for steady wall effects. Both methods are restricted to low aspect ratio models and to low reduced frequencies (quasi-steady flow).

3D wall correction by application of the integral equation method described in the previous sections for 2D flow will need a great number N of panels for representation of the walls (typically several hundred), thus demanding vast computer storage space ($\sim N^2$) for the calculation of the aerodynamic influence coefficients and long computing time ($\sim N^3$) for inversion of the influence matrices.

A significant simplification, especially for complex wind tunnel models, might be possible by neglecting in Eqs. (6.16) and (6.17) those terms which simulate the model. In Ref. [23] ASHILL and KEATING have shown for steady subsonic wall interference that this simplification is justified if equivalent free stream velocities and model shapes can

be defined. An alternative would be the use of finite difference methods. But in this case, the formulation of the unsteady problem in terms of the Helmholtz equation is not adequate because it would introduce severe numerical difficulties. In Ref. [24] it has been shown, that for finite difference solution of Eq. (3.6) or Eq. (6.15) a limited upper reduced frequency exists. Relaxation methods converge only below this limit. For the wind tunnel problem its value just equals the lowest tunnel resonance frequency.

This difficulty can be overcome by formulation of the problem in the time domain (such as Eq. (3.1) and Eq. (3.2)) and then application of ADI-solution methods. Assuming again validity of a linearized unsteady potential equation (subsonic or transonic time linearization), the difference between free stream and wind tunnel flow also satisfies this equation. For example in 2D subsonic flow the potential correction $(\phi^J - \phi)$, based on Eq. (3.1), is

$$(6.18) \quad \frac{\partial^2}{\partial \overline{x}^2}(\phi^J - \phi) + \frac{\partial^2}{\partial \overline{y}^2}(\phi^J - \phi) - 2\frac{M_\infty^2}{\beta^2}\frac{\partial^2}{\partial \overline{x}\partial T}(\phi^J - \phi) - \frac{M_\infty^2}{\beta^2}\frac{\partial^2}{\partial T^2}(\phi^J - \phi) = 0.$$

While boundary conditions at the model are unchanged by wall effects, thus yielding zero downwash for the potential correction, the other boundary conditions have to be formulated carefully. For the free stream case non-reflecting boundary conditions, as given in Refs. [25] and [26], have to be used at the walls as well as on upstream and downstream boundaries. For the subsonic problem these boundary conditions read

$$(6.19) \quad \frac{\partial \phi^J}{\partial \overline{y}} \pm \frac{M_\infty^2}{1 - M_\infty^2}\frac{\partial \phi^J}{\partial T} = 0 \quad \text{for} \quad \overline{y} \gtrless 0.$$

For closed tunnel walls we have

$$\frac{\partial \phi}{\partial \overline{y}} = 0, \quad \phi = \phi^W \quad \text{(experimental)}.$$

This yields following boundary conditions for the correction potential $(\phi^J - \phi)$

$$(6.20) \quad \frac{\partial}{\partial \overline{y}}(\phi^J - \phi) \pm \frac{M_\infty^2}{1 - M_\infty^2}\frac{\partial}{\partial T}(\phi^J - \phi) = \pm\frac{M_\infty^2}{1 - M_\infty^2}\frac{\partial \phi^W}{\partial T}$$

at walls.

It is clear that such 3D unsteady wall correction techniques based on experimentally determined wall boundary conditions may presently appear rather prospective. However, with the further development of 3D adaptive wall concepts together with further improvements in CFD methods, such hybrid wind tunnel wall correction techniques may soon reach maturity.

7. Concluding remarks

Adaptive wind tunnel walls, already successfully applied to eliminate steady flow wall interference, cannot readily be applied in the same manner to (motion-induced) unsteady flow fields. Even in the case of 2D unsteady flow, wall adaptation would require tremendous technical effort: 3D adaptive walls for unsteady flow fields lie beyond the realm of practicability. However, as unsteady aerodynamic processes may also strongly be affected by steady flow wall interference, application of steady flow wall adaptation would also considerably improve unsteady aerodynamic wind tunnel test results. Thus, steady flow wall adaptation with the possibility to measure also (after the steady flow adaptation)

unsteady wall pressure data, together with the application of advanced CFD-techniques which take the measured unsteady wind tunnel wall data into account in formulating precise tunnel wall boundary conditions, is most promising in the development of new numerical techniques for correction of wall interference in unsteady flow. Elaboration of such hybrid correction techniques, and their experimental verification by corresponding systematic wind tunnel measurements, is a challenging field of future aerodynamic research. It would contribute substantially to a new generation of advanced wind tunnel technology.

Acknowledgement

References

1. U. GANZER, *Advances in adaptive wall wind tunnel techniques*, in: Recent Advances in Aerodynamics and Aeroacoustics, pp. 567–601, Springer Verlag, Berlin 1984.
2. W. R. SEARS, J. C. ERICKSON, *Adaptive wind tunnels*, Ann. Rev. Fluid Mech., **20**, pp. 17–34, 1988.
3. E. H. DOWELL, *Control laws for adaptive wind tunnels*, AIAA J., **19**, 11, pp. 1486–1488, November 1981.
4. E. WEDEMEYER, A. HEDDERGOTT and D. KUCZKA, *Deformable adaptive wall test section for 3D wind tunnel testing*, J. Aircraft, **22**, 12, 1985.
5. S. BODAPATI, E. SCHAIRER and S. DAVIS, *Adaptive-wall wind tunnel development for transonic testing*, AIAA Paper, 80–0441, March 1980.
6. M. T. LANDAHL, *Unsteady transonic flow*, Pergamon Press, 1961.
7. S. R. BLAND, *The two-dimensional oscillating airfoil in a wind tunnel in subsonic flow*, SIAM J. Appl. Math., **18**, pp. 830–848, 1970.
8. J. A. FROMME and M. A. GOLBERG, *Unsteady two-dimensional airloads acting on oscillating thin airfoils in subsonic ventilated wind tunnels*, NASA CR, 2967, 1978.
9. J. A. FROMME and M. A. GOLBERG, *Aerodynamic interference effects on oscillating airfoils with controls in ventilated wind tunnels*, AIAA J., **18**, pp. 417–426, 1980.
10. H. C. GARNER, *Theoretical use of variable porosity in slotted tunnels for minimizing wall interference on dynamic measurements*, ARC R and M, 3706, 1971.
11. M. F. PLATZER, *Wind tunnel interference on oscillating airfoils in low supersonic flow*, Acta Mechanica, **16**, pp. 115–126, 1973.
12. H. SAWADA, *A new method of estimating wind tunnel wall interference in unsteady two-dimensional flow*, NRC, 21274, 1983.
13. H. L. RUNYAN and C. E. WATKINS, *Consideration on the effect of wind tunnel walls on oscillating air forces for two-dimensional subsonic compressible flow*, NACA Report, 1150, 1951.
14. H. L. RUNYAN, D. S. WOOLSTON and A. G. RAINEY, *Theoretical and experimental investigation of the effect on tunnel walls on the forces on an oscillating airfoil in two-dimensional subsonic compressible flow*, NACA Report, 1262, 1955.
15. D. G. MABEY, *Resonance frequencies of ventilated wind tunnels*, AIAA J., **18**, pp. 7–8, 1980.
16. D. G. MABEY, *The reduction of dynamic interference by sound-absorbing walls in the RAE 3 ft. wind tunnel*, RAE TR, 77120, 1977.
17. D. KUCZKA, *Hybridverfahren für instationäre Messungen in transsonischen Windkanälen am Beispiel der harmonischen Nickschwingung*, DFVLR-FB 88–19, 1988.
18. C. POSSIO, *L' azione aerodinamica sul profilo oscillante in un fluido compressibile a velocita iposonora*, L'Aerotechnica, 18, pp. 441–458, 1938.
19. R. VOSS, *Instationäre Windkandwald-Interferenzen bei sub- und transsonischer Profilumströmung*, Festschrift zum 60. Geburtstag von Prof. Dr. H. Försching, DLR-Inst. für Aeroelastic, Göttingen, pp. 169–185, 1990.
20. M. A. JONES, *Wind-tunnel wall interferences effects on oscillating airfoils in subsonic flow*, ARC R and M, 2943, 1953.

21. W. Geissler and R. Voss, *Investigations of the unsteady airloads with oscillating control in sub- and transonic flows*, in: Proc. 1st Int. Symp. on Aeroelasticity, DGLR Report, 82–01, 1982.

22. H. C. Garner, *The theory of interference effects on dynamic measurements in slotted-wall tunnels at subsonic speeds and comparisons with experiment*, ARC R and M, 3500, 1968.

23. P. R. Ashill and R. F. A. Keating, *Calculation of tunnel wall interference from wall-pressure measurements*, RAE TR, 85086, 1985.

24. F. E. Ehlers and W. H. Weatherill, *A harmonic analysis method for unsteady transonic flow and its application to the flutter of airfoils*, NASA CR, 3537, 1982.

25. B. Engquist and A. Majda, *Radiation boundary conditions for acoustic and elastic wave calculations*, Comm, Pure and Appl. Math., **32**, pp. 313–357, 1979.

26. D. Kwak, *Non-reflecting far-field boundary conditions for unsteady transonic flow computation*, AIAA J., **19**, pp. 1401–1407, 1981.

DLR-INSTITUTE OF AEROELASTICITY, GÖTTINGEN, GERMANY.